

## Evidence for quantum-confined Stark effect in GaN/AlN quantum dots in nanowires

J. Renard,<sup>1</sup> R. Songmuang,<sup>1</sup> G. Tourbot,<sup>2</sup> C. Bougerol,<sup>1</sup> B. Daudin,<sup>1</sup> and B. Gayral<sup>1,\*</sup><sup>1</sup>CEA-CNRS Group "Nanophysique et Semiconducteurs," INAC/SP2M, and Institut Néel/CNRS, Université J. Fourier-CEA Grenoble, 17 rue des Martyrs, 38054 Grenoble, France<sup>2</sup>CEA-LETI, MINATEC, 17 rue des Martyrs, 38054 Grenoble Cedex 9, France

(Received 22 July 2009; revised manuscript received 25 August 2009; published 17 September 2009)

Semiconductor nanowires have the potential to outperform two-dimensional structures, for instance for light-emitting applications. However, the intrinsic fundamental properties of heterostructures in nanowires still remain to be assessed and compared to their two-dimensional counterparts. We show that polar GaN/AlN axial heterostructures in nanowires grown by plasma-assisted molecular-beam epitaxy are subject to a clear quantum-confined Stark effect. However, the magnitude of this effect is smaller than for two-dimensional structures due to the reduction in piezoelectric polarization that occurs thanks to elastic relaxation which is favored by the nanowire free surfaces. Moreover, we show by temperature-dependent photoluminescence measurement and single-photon correlation measurements that these heterostructures behave like quantum dots.

DOI: [10.1103/PhysRevB.80.121305](https://doi.org/10.1103/PhysRevB.80.121305)

PACS number(s): 78.67.Hc, 78.55.Cr, 77.65.Ly

GaN nanowires (NWs) can be grown spontaneously by plasma-assisted molecular-beam epitaxy (PA-MBE) under nitrogen-rich conditions.<sup>1</sup> While two-dimensional (2D) III-N layers grown on heterosubstrates show large dislocation densities, III-N NWs hold the promise to realize heterostructures that are free of defects due to surface strain relaxation. This is particularly true for axial heterostructures for which the critical thickness for plastic relaxation can be much larger than for two-dimensional layers.<sup>2</sup> While this is appealing for potential light-emitting applications, fundamental properties of heterostructures embedded in III-N NWs have not yet been studied in depth. First, it is not clear whether such axial heterostructures behave like quantum wells (QWs) or quantum dots (QDs). The typical diameter of III-N NWs grown by PA-MBE is in the 20–50 nm range, which is large compared to the GaN Bohr radius (3 nm). Due to this weak lateral confinement, such heterostructures are coined as quantum wells, quantum dots, or quantum disks. We will use either of these terms in this Rapid Communication when discussing the literature, and we will show experimental evidence that these heterostructures behave rather like QDs. Second, one might wonder whether the quantum-confined Stark effect (QCSE)—which plays a major role in the optical properties of polar two-dimensional III-N heterostructures—is also present in axial heterostructures inserted in PA-MBE grown III-N NWs (for which the NWs grow along the *c* axis). Although many papers have been published on heterostructures in wurtzite NWs, a large QCSE has never been clearly demonstrated in such structures. Let us recall that the QCSE leads to a redshift of the heterostructure transitions and a strong reduction in the oscillator strength. In particular the observation of a QW emission at energies below the band gap of the QW material is an unambiguous demonstration of the QCSE.<sup>3,4</sup> For NWs, it is possible to argue that the particular heterostructure geometry might lead to a reduction in the QCSE, notably due to the strain relaxation that reduces the piezoelectric component of the polarization difference. In fact for InGaN/GaN QWs in NWs, Kawakami and co-workers showed by time-resolved photoluminescence (PL) that the QCSE is strongly reduced in

NWs compared to two-dimensional QWs emitting in the same spectral region.<sup>5</sup> A similar analysis was done on InGaN/GaN NWs light-emitting diode structures<sup>6</sup> and in both cases the reduction in the QCSE was attributed to a reduction in the piezoelectric polarization in NWs. For GaN/AlGaIn structures, the authors of Refs. 7 and 8 studied GaN/AlGaIn quantum disks in NWs. They emphasize that the main confinement mechanism is what they call “strain confinement” due to inhomogeneous strain relaxation along the wire diameter. They nonetheless take into account the QCSE in their calculation and show slightly below band-gap emission for the thickest disks (4 nm) and the largest Al composition (30%). In particular Rivera *et al.* showed time-resolved photoluminescence data that convincingly demonstrate the oscillator strength reduction for thicker disks.<sup>8</sup> We also note that the precise AlGaIn composition and homogeneity in NWs are not well known, notably due to a lack of knowledge on the ternary alloy disorder in such NW structures.

We hereafter present a study of the fundamental properties of GaN/AlN axial heterostructures in NWs. We first demonstrate a large QCSE for these structures, in particular with a QD emission at energies well below the GaN band gap. We then highlight and discuss the quantitative difference of the QCSE magnitude with what is observed for Stranski-Krastanow QDs. We finally demonstrate that these structures behave like QDs.

Samples were grown on (111) Si substrates by radio frequency PA-MBE under N-rich atmosphere. After standard degreasing followed by etching in HF (5%) for 2 min, the substrate was thermally outgassed in the growth chamber until appearance of a (7×7) reconstruction, characteristic of clean Si (111) surface. A thin 2D AlN buffer layer was grown on Si substrate prior to GaN deposition in order to improve the wire orientation.<sup>9</sup> The samples consisted of a base of GaN NWs, between 500 and 700 nm long. Next, after the growth of GaN NWs, about 10 nm of AlN was deposited in N-rich conditions. Single insertions of GaN were grown on top of the AlN section using the same experimental conditions as for the GaN NWs. Their nominal thickness was pro-

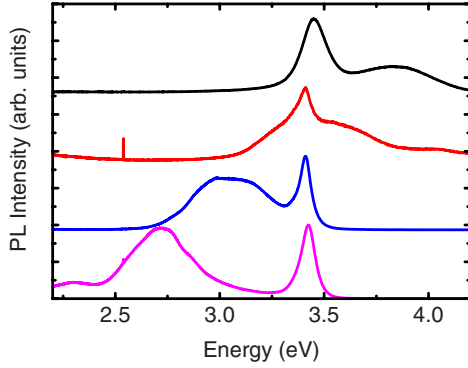


FIG. 1. (Color online) Room-temperature macroPL spectra of ensembles of NWs containing single GaN/AlN axial heterostructures with varying QD height. The peak around 3.45 eV stems from the GaN base of the wire. The broad peak from the QD luminescence shifts toward small energies for thicker GaN QDs.

portional to deposition time and ranged from 1 to 4 nm. They were covered by an upper AlN barrier, about 10 nm thick. A schematic of the grown structures can be found in Ref. 10. A sample with 10 GaN insertions separated by 10 nm AlN barriers was also grown.

The macrophotoluminescence spectra were obtained by exciting the samples with a continuous wave frequency-doubled argon laser emitting at 244 nm, at low excitation power density (around  $0.1 \text{ W cm}^{-2}$ ). The microphotoluminescence spectra were obtained by focusing this same laser to a spot of about  $1 \text{ } \mu\text{m}$  in diameter with a refractive microscope objective (numerical aperture 0.4). Finally the time-resolved data were obtained by exciting the sample with a frequency-tripled Ti:sapphire laser (pulse duration 200 fs and pulse frequency 76 MHz) and analyzing the PL with a streak camera.

Figure 1 shows the room-temperature PL for the various samples of QDs in NWs with different nominal thicknesses.

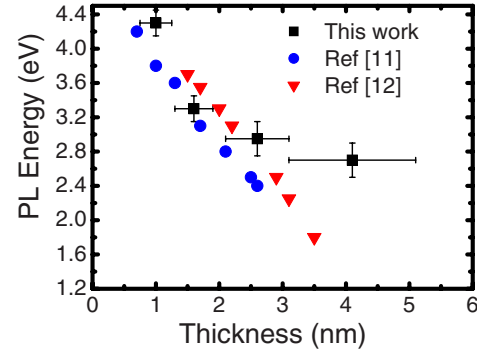


FIG. 3. (Color online) PL energy (at room temperature) as a function of QD or QW thickness for this work (PL data from Fig. 1) and other references. The error bars correspond to the PL broadening (full width at half maximum) and to the measured QD thickness dispersion.

The signal around 3.4–3.45 eV is due to the GaN base of the NW. The PL of the ensemble of QDs shows a monotonic evolution of its spectral position as a function of QD thickness. In particular, for the thickest QDs, the luminescence occurs at energies well below the GaN band gap with a peak around 2.7 eV. This shows unambiguously that for the largest QDs, the carrier confinement is dominated by the QCSE.

The next step consists in estimating the QD height in the various samples so as to be able to correlate the spectral position of the emission with the QD thickness. For this purpose, we have performed high-resolution transmission electron microscopy (TEM) on several NWs of each sample. Figure 2 shows two examples of GaN QDs in NWs with thicknesses 1.5 and 4.5 nm. This then allows us to plot the peak transition energy of the QDs as a function of the measured QD heights, as represented in Fig. 3. The error bars on the QD thicknesses are due to the dot to dot variations in the measured heights for a given sample. The trend shows a decrease in the transition energy with increasing QD height,

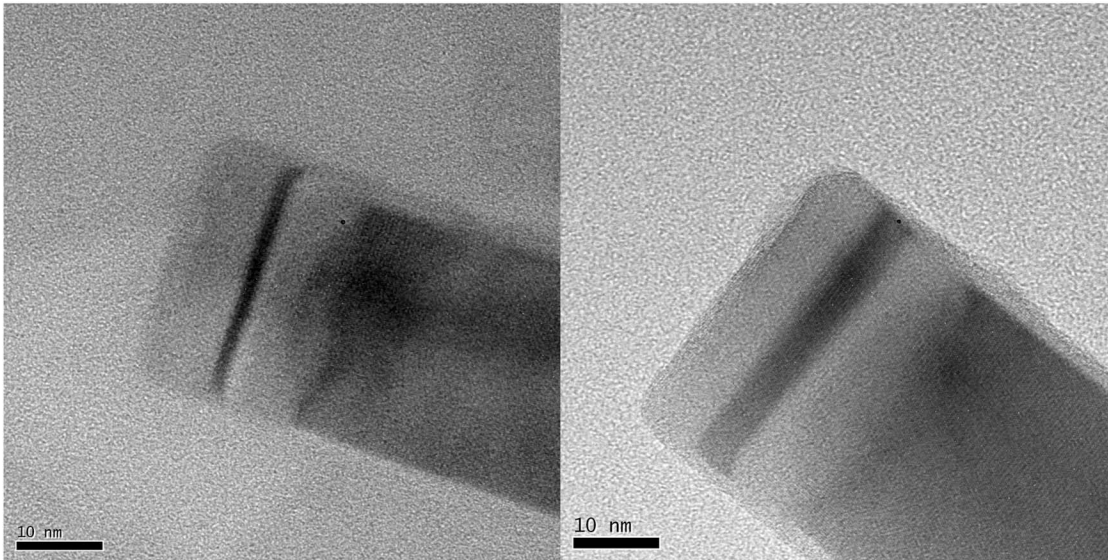


FIG. 2. High-resolution TEM pictures from GaN/AlN heterostructures in NWs. In both cases the scale bar is 10 nm. The thicknesses of the GaN QDs are 1.5 (left) and 4.5 nm (right).

however, with a slow down for the larger thicknesses. It is then interesting to compare such data with what occurs for Stranski-Krastanow (SK) GaN/AlN QDs. While there is unfortunately no similar experimental study for SK QDs that links the PL peaks to the measured QD heights in the 1–4 nm range, this issue has been addressed for QWs,<sup>11</sup> and it is well known that SK GaN QDs behave similarly to QWs of similar height. Concerning QDs, the height versus fundamental transition energy has been modeled by several groups, and we take as comparison the model by Bretagnon *et al.*<sup>12</sup> which has been validated by time-resolved data. It appears that the decrease in the luminescence peak as a function of QD thickness keeps a constant slope over the considered range, while a weaker size dependence is observed for QDs in NWs (see Fig. 3). We tentatively attribute this reduction in the QCSE for the thicker dots in NWs to a decrease in the piezoelectric field due to a strain relaxation. Qualitatively, it is indeed expected that for thin GaN/AlN insertions, the GaN will be globally strained by the AlN below and above (which is expected to be relaxed) while for thicker insertions, the NW geometry will allow the GaN to relax through lateral surfaces. In the latter case, the piezoelectric component of the polarization will be suppressed so that the QCSE will only be due to the spontaneous polarization difference. For polar GaN/AlN heterostructures, this leads to an overall reduction in the polarization difference and hence to a reduction in the QCSE, which occurs in our case for QDs with heights larger than 2 nm. This explanation ought to be confirmed by further experimental and theoretical work taking into account the precise strain profile in the NW structure and also possibly taking into account other effects such as surface band bending as evoked in Ref. 5.

The next issue we address is to probe whether these axial heterostructures really behave like QDs. In particular, one key issue is their radiative efficiency and the possible existence of nonradiative channels due to the NW geometry (surface recombinations for instance). A way to probe these effects is to study the temperature dependence of the PL and time-resolved PL. In our structures, at low temperature, the main part of the signal comes from the GaN base of the NWs, and we could thus carry out a detailed study only for the smallest QDs (the PL of the larger QDs has a too strong overlap with the GaN near band-edge signal to be able to extract reliable time-resolved data). The results are presented in Fig. 4. If one assumes that the efficiency is 100% at low temperature, the integrated intensity gives a value of 50% for the room-temperature internal efficiency. The inset displays the decay time and integrated luminescence intensity variations as a function of temperature. While the decay of the PL is not monoexponential, the  $1/e$  decay time is nearly constant between 4 K and room temperature (around 300 ps). This proves that thermally activated nonradiative recombination processes are negligible up to room temperature. This is thus a QD-like behavior,<sup>13</sup> especially for GaN/AlN structures for which the PL of QWs quenches dramatically with raising temperature.<sup>14</sup> Beyond this remarkable temperature behavior—which is essential for potential applications—the ultimate proof that a semiconductor emitter is a QD with well-separated discrete levels consists in showing the antibunching behavior of the emitted PL.<sup>15</sup> Concerning III-N

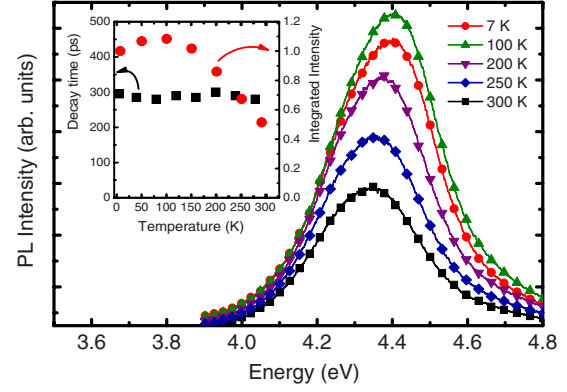


FIG. 4. (Color online) MacroPL spectra for GaN/AlN QDs in NWs as a function of sample temperature. Each NW contains 10 QDs separated by 10 nm AlN barriers. This sample was used to increase the PL signal and obtain better experimental data. We checked that NWs containing several QDs and single QDs behave in the same way. The inset displays the decay time at  $1/e$  and the integrated PL intensities as a function of temperature.

QDs in NWs, the PL of single insertions was probed in the GaN/AlN system<sup>10</sup> and in the InGaN/GaN system<sup>16</sup> and in both cases sharp lines were observed, with the identification of single exciton and biexciton transitions. This already gives a good hint that localized discrete states are probed but does not demonstrate fully that a single discrete level is observed. We have performed a Hanbury-Brown and Twiss-type measurement of the second-order correlation function [ $g_2(t)$ ] of the photon stream emitted by a single GaN/AlN QD in a NW under continuous wave excitation,<sup>15</sup> the emission being around 4 eV (see Ref. 10 for the experimental procedure of single NW microPL). The obtained histogram is represented in Fig. 5. The antibunching dip reaches a value smaller than 0.5, thus demonstrating the single discrete level character of the emitter. Note that the measured value of 0.4 can be fully accounted for when taking into account the limited time-resolution of the single-photon detectors that were used in the framework of a Monte Carlo model describing the excitation-decay mechanism.

In conclusion, we have clearly shown that GaN/AlN axial heterostructures are subject to the quantum-confined Stark

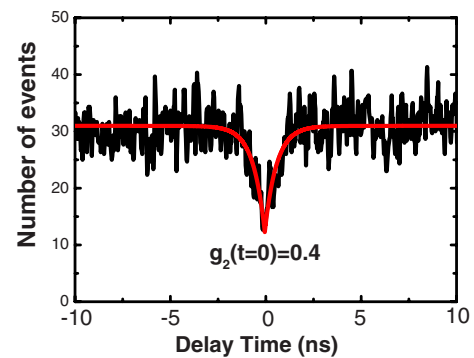


FIG. 5. (Color online) Hanbury-Brown and Twiss coincidence histogram for the PL at 4 K of a single GaN/AlN QD in a NW. The continuous line is a fit of the experimental data that allows us to extract  $g_2(t=0)$ .



effect although its magnitude is in that case less than for two-dimensional equivalent structures. We attribute this to the favored elastic strain relaxation in NWs. We have furthermore demonstrated that such heterostructures—despite their quite large diameter—do behave like QDs, both concerning the robustness of the PL with temperature and the discreteness of their confined levels as probed by second-order correlation measurements.

The authors acknowledge fruitful discussions with D. Camacho Mojica and Y.-M. Niquet. They also acknowledge financial support from French National Agency (ANR) through Carnot funding and project BONAFO Grant No. ANR-08-NANO-031-01. We thank G. Tarel and V. Savona (EPFL, Switzerland) for sharing with us their insight on Monte Carlo simulation of second-order correlation measurements before publication.

\*bruno.gayral@cea.fr

- <sup>1</sup>M. A. Sanchez-Garcia, E. Calleja, E. Monroy, F. J. Sanchez, F. Calle, E. Munoz, and R. J. Beresford, *J. Cryst. Growth* **183**, 23 (1998).
- <sup>2</sup>F. Glas, *Phys. Rev. B* **74**, 121302(R) (2006).
- <sup>3</sup>M. Leroux, N. Grandjean, M. Lügt, J. Massies, B. Gil, P. Lefebvre, and P. Bigenwald, *Phys. Rev. B* **58**, R13371 (1998).
- <sup>4</sup>V. Fiorentini, F. Bernardini, F. Della Sala, A. Di Carlo, and P. Lugli, *Phys. Rev. B* **60**, 8849 (1999).
- <sup>5</sup>Y. Kawakami, S. Suzuki, A. Kaneta, M. Funato, A. Kikuchi, and K. Kishino, *Appl. Phys. Lett.* **89**, 163124 (2006).
- <sup>6</sup>C. Y. Wang, L. Y. Chen, C. P. Chen, Y. W. Cheng, M. Y. Ke, M. Y. Hsieh, H. M. Wu, L. H. Peng, and J. J. Huang, *Opt. Express* **16**, 10549 (2008).
- <sup>7</sup>J. Ristic, C. Rivera, E. Calleja, S. Fernández-Garrido, M. Povoloskyi, and A. Di Carlo, *Phys. Rev. B* **72**, 085330 (2005).
- <sup>8</sup>C. Rivera, U. Jahn, T. Flissikowski, J. L. Pau, E. Muñoz, and H. T. Grahn, *Phys. Rev. B* **75**, 045316 (2007).
- <sup>9</sup>R. Songmuang, O. Landré, and B. Daudin, *Appl. Phys. Lett.* **91**,

251902 (2007).

- <sup>10</sup>J. Renard, R. Songmuang, C. Bougerol, B. Daudin, and B. Gayral, *Nano Lett.* **8**, 2092 (2008).
- <sup>11</sup>C. Adelmann, E. Sarigiannidou, D. Jalabert, Y. Hori, J.-L. Rouvière, B. Daudin, S. Fanget, C. Bru-Chevallier, T. Shibata, and M. Tanaka, *Appl. Phys. Lett.* **82**, 4154 (2003).
- <sup>12</sup>T. Bretagnon, P. Lefebvre, P. Valvin, R. Bardoux, T. Guillet, T. Taliencio, B. Gil, N. Grandjean, F. Semond, B. Damilano, A. Dussaigne, and J. Massies, *Phys. Rev. B* **73**, 113304 (2006).
- <sup>13</sup>F. Widmann, B. Daudin, G. Feuillet, Y. Samson, J. L. Rouvière, and N. Pelekanos, *J. Appl. Phys.* **83**, 7618 (1998).
- <sup>14</sup>M. Furis, A. N. Cartwright, H. Wu, and W. J. Schaff, *Appl. Phys. Lett.* **83**, 3486 (2003).
- <sup>15</sup>P. Michler, A. Imamoglu, M. D. Mason, P. J. Carson, G. F. Strouse, and S. K. Buratto, *Nature (London)* **406**, 968 (2000).
- <sup>16</sup>R. Bardoux, A. Kaneta, M. Funato, Y. Kawakami, A. Kikuchi, and K. Kishino, *Phys. Rev. B* **79**, 155307 (2009).